J. Phys.: Condens. Matter 4 (1992) 5239–5248. Printed in the UK

The effect of absorbed hydrogen on the amorphization of CuTi alloys

P K Ivison†, I Soletta‡, N Cowlam†, G Cocco‡, S Enzo§ and L Battezzati¶

† Department of Physics, University of Sheffield, Sheffield S3 7RH, UK
‡ Dipartimento di Chimica, Università di Sassari, via Vienna 2, 07100 Sassari, Italy
§ Dipartimento di Chimica Fisica, Università di Venezia, Calle Larga, S Marta 2137, 30123 Venice, Italy
¶ Dipartimento di Chimica Inorganica, Chimica Fisica e Chimica dei Materali, Università di Torino, via P Giuria 9, 10125 Turin, Italy

Received 15 January 1992, in final form 26 March 1992

Abstract. Neutron and x-ray diffraction measurements have been made on a series of amorphous CuTi alloys produced by mechanical alloying (MA). Parent titanium powder was used that was free from hydrogen. The copper-rich alloys were found to be fully amorphous after 16 hours of MA, but the reaction was incomplete in the titanium-rich alloys after the same period and they consisted of intermetallic phases. This is in contrast with the results for a series of samples examined by us previously, which had small contaminations of hydrogen, but which all transformed to an amorphous state after the same period of MA. This suggests that the presence of hydrogen stimulates the amorphization reaction and that in its absence the reaction is inhibited in the titanium-rich samples. It is also found that the degree of chemical short-range order present in the fully transformed amorphous samples is also influenced by the hydrogen contamination in the parent titanium.

1. Introduction

We have recently examined a series of amorphous copper titanium alloys produced by mechanical alloying (MA) using x-ray and neutron diffraction (Ivison *et al* (1991b), hereafter referred to as I). The aim of this work was to establish the significance of chemical short-range order (CSRO) in the amorphization reaction. However, evidence was found in the neutron diffraction patterns of a small degree of hydrogen contamination in these alloys, which was not detected in the routine x-ray diffraction measurements made to check the state of the samples after the MA process. This contamination was estimated to be 15 at.% in the parent titanium which reduced to between 4 and 10% on the actual CuTi specimens. After suitable corrections had been made to the diffraction patterns, total structure factors $S(Q)$ were obtained that showed that these samples were truly amorphous. These $S(Q)$ resembled those of CuTi glasses (Sakata *et al* 1982) and of CuTi molten alloys (He Fenglai *et al* 1986) examined by us in the past. The normalized height of the pre-peak in $S(Q)$ was taken as a measure of the degree of CSRO present. The values for the MA samples lay below those of the metallic glasses and were comparable with those for the molten state. We have now taken the opportunity of examining a new series of CuTi samples,

0953-8984/92/235239+10$04.50

made using uncontaminated titanium powder, during a second allocation of experimental time on the D20 diffractometer at ILL Grenoble. In this paper we will report the rather unexpected observation that the *absence* of hydrogen appears to inhibit the amorphization reaction in the titanium-rich alloys.

2. Sample preparation and experimental method

The preparation of the samples and the diffraction experiments followed the same procedures as described in the previous paper (I), except that for the new specimens, 325-mesh titanium powder of 2N purity supplied by ALPHA was used, instead of the titanium powder supplied by VENTRON. Seven samples were produced over the same composition range as the original samples (75–30 at.% copper) and the milling time for each was 16 hours, the same as for all but one of the first series. The first indication that there was a different outcome in the MA treatment, was provided by the routine x-ray measurements through the first broad diffraction halo, seen in figure 1. It was observed that alloys with less than 50 at.% titanium gave a diffuse halo of the expected form, but for the $Cu_{45}Ti_{55}$, $Cu_{40}Ti_{60}$ and $Cu_{30}Ti_{70}$ samples, broadened Bragg peaks from crystalline phases were superimposed.

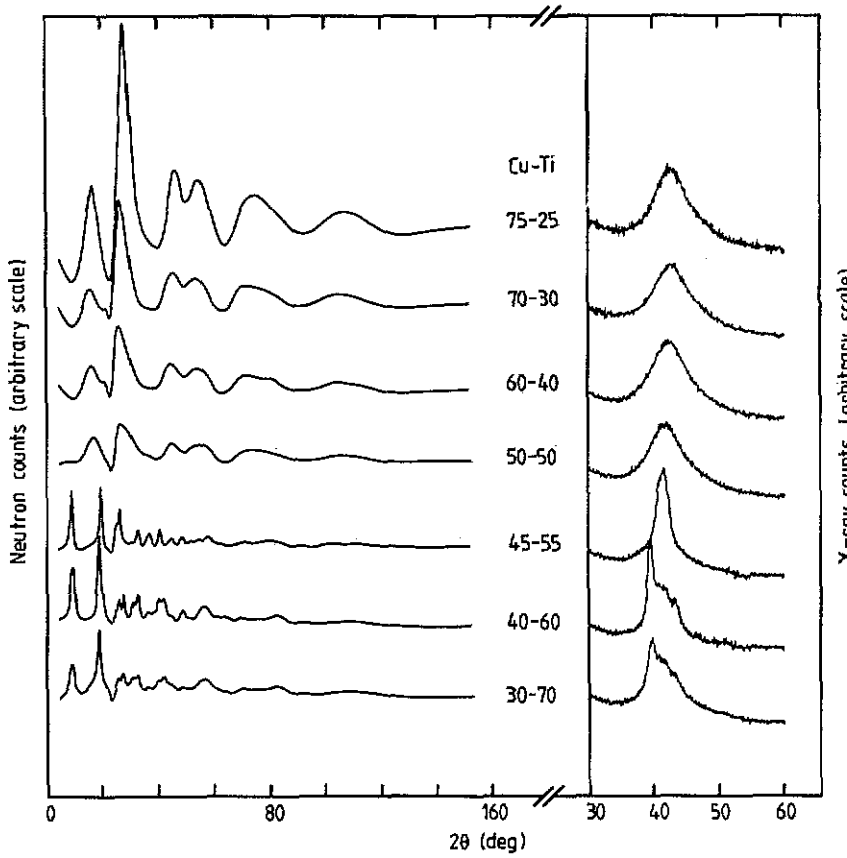

Figure 1. Neutron diffraction patterns of the seven Cu_xTi_{100-x} MA samples are shown. The exploratory x-ray diffraction scans through the first broad halo are shown on the right of the figure. 2θ is the scattering angle.

The neutron experiments were as close to the original measurements as possible. The diffraction patterns for the seven samples are shown in figure 1. They illustrate immediately that the samples are essentially hydrogen free—by the absence of the high sloping background due to incoherent neutron scattering from hydrogen that was observed in the previous study (see figure 1 of I, for comparison). However, the most important feature of the neutron, as opposed to the x-ray result, is the clear indication of sharp Bragg peaks in the diffraction patterns of the three titanium-rich samples, out to a scattering angle of $2\theta \simeq 60°$. Close inspection of these patterns shows additional diffuse contributions from an amorphous phase. Note that because the angular ranges of the neutron and x-ray data are different this gives a slightly false impression of the resolution of the two instruments. The peak half-widths for the $Cu_{50}Ti_{50}$ are, in fact, about 8° of 2θ for both radiations. However, the reasons for the rather large apparent differences between the x-ray and neutron diffraction patterns taken for the same sample materials will be discussed more fully below.

3. Atomic scale structures of mechanically alloyed Cu_xTi_{100-x}

It is convenient to divide the alloys examined into two groups either side of the equiatomic composition.

3.1. Amorphous CuTi alloys

The total structure factors $S(Q)$ have been obtained for the four copper-rich specimens using the methods described previously (I) with the exception, of course, of the correction for scattering from hydrogen. The $S(Q)$ curves derived are similar to those of the other disordered CuTi alloys obtained before (e.g. in I) and all have the characteristic pre-peak at $Q = 1.9$ Å^{-1} and main peak at $Q \simeq 3$ Å^{-1}. Figure 2 shows the $S(Q)$ curves for the present MA specimens with the equivalent curves for copper-rich CuTi metallic glasses (Sakata *et al* 1982) given as an inset. Figure 3 shows the $S(Q)$ for just the copper-rich examples from the hydrogen-contaminated MA series investigated previously (I) with the equivalent curves for copper-rich CuTi molten alloys (He Fenglai *et al* 1986) given as an inset. It is clear, by comparing the results for samples of the same composition, that the pre-peak is higher for the hydrogen-free samples (figure 2) than in the contaminated samples (figure 3) and that the features of the $S(Q)$ are generally better resolved in the region of the second split peak (5–6 Å^{-1}). To quantify the degree of CSRO present in these samples requires, at the minimum, a determination of the Bhatia and Thornton (1970) partial structure factors (PSF), $S_{NN}(Q)$ and $S_{CC}(Q)$, and work on this is in progress. However, since there is ample evidence (Sakata *et al* 1982, Fukunaga *et al* 1984, Ruppersberg *et al* 1980, Blètry 1978) that the pre-peak in $S(Q)$ can be associated with the PSF $S_{CC}(Q)$ describing CSRO (Bhatia and Thornton 1970) in the absence of a more detailed analysis, its height relative to the main peak can be used to estimate the degree of CSRO present. A ratio R_N, normalized by the weighting factors W_{NN} and W_{CC} of the Bhatia and Thornton (1970) PSFs, can be used as previously in (I):

$$R_N = \frac{\text{Height of pre-peak}/W_{CC}}{\text{Height of main peak}/W_{NN}}.$$

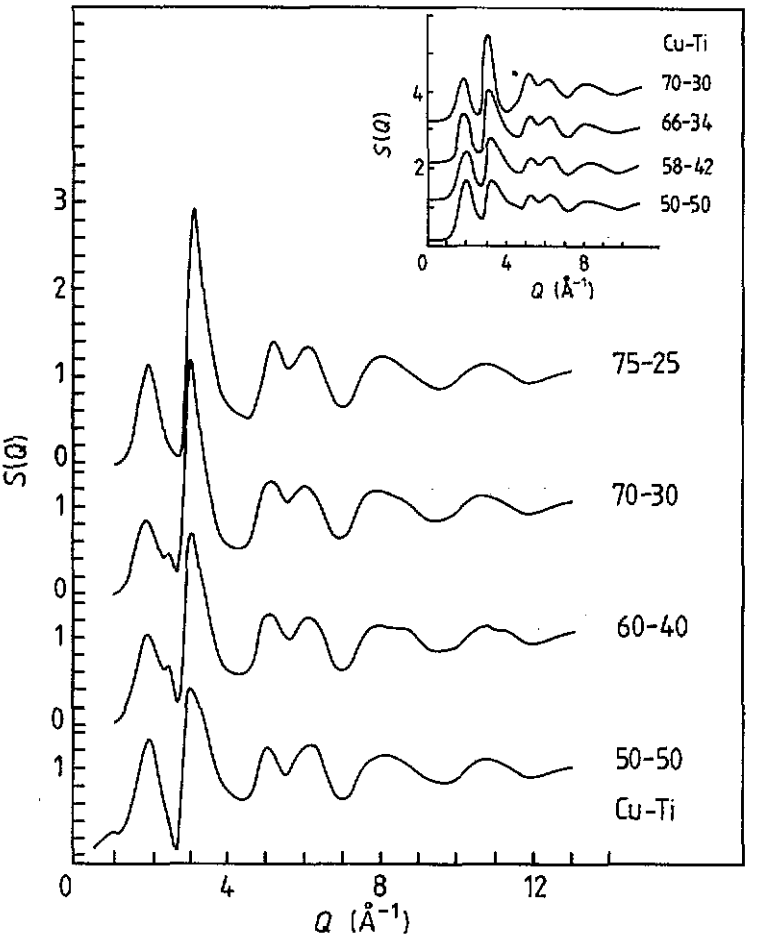

Figure 2. The structure factors $S(Q)$ for the four copper-rich Cu_xTi_{100-x} MA samples derived from the curves given in figure 1 are shown. The $S(Q)$ curves for copper-rich Cu_xTi_{100-x} metallic alloy glasses (after Sakata *et al* 1982) are given in the inset. Q is the scattering vector.

The values of R_N for all the CuTi alloys examined to date are given in table 1 and plotted in figure 4. These graphs show that the values of R_N, and presumably CSRO, vary with composition. In the case of the metallic glasses and the molten alloys this probably reflects the presence of strong unlike-atom correlations which are responsible for the eutectic minima in the CuTi phase diagram. The magnitudes of R_N for the MA samples and their variation in figure 4(*b*) confirm the impression given by figures 2 and 3 that the $S(Q)$ of the hydrogen-free MA alloys are similar to those of the CuTi metallic glasses while the $S(Q)$ of the hydrogen-contaminated MA alloys are similar to those of molten CuTi alloys. Thus a conclusion of this simple comparison is that CSRO is better developed in the present hydrogen-free samples than in the hydrogen-contaminated ones examined previously (I).

In the previous study (I) it was explained how the Fourier transforms of these total $S(Q)$ curves can be presented either as a radial distribution function (RDF) when the Bhatia and Thornton (1970) weighting factor W_{NN} is large or as a radial

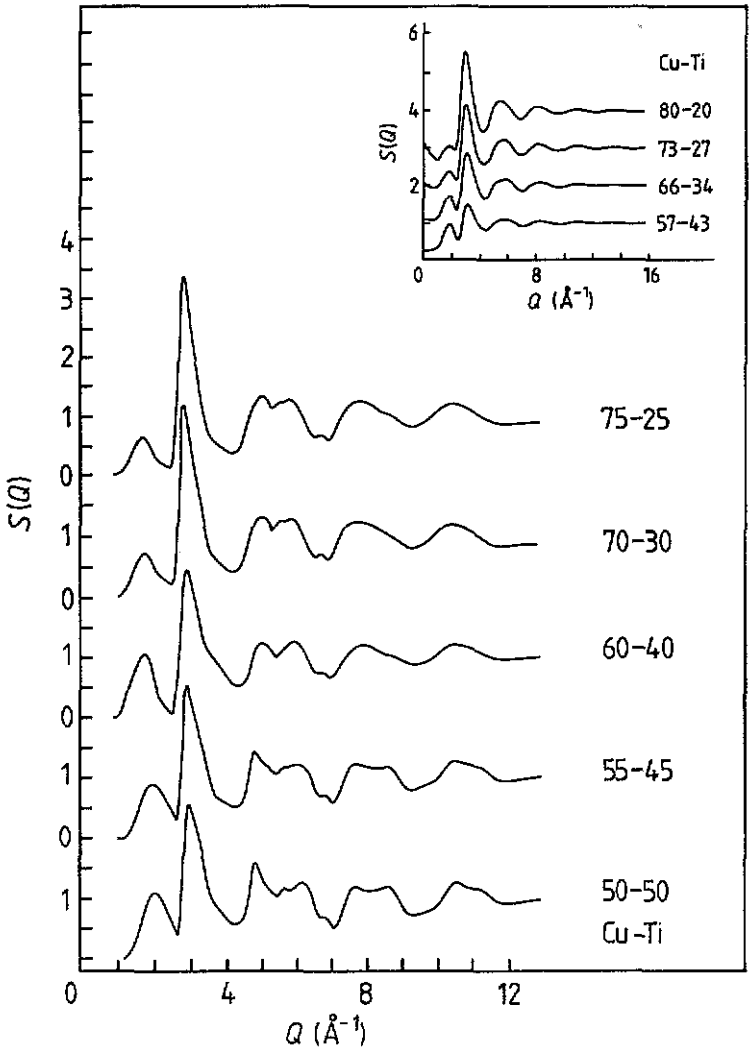

Figure 3. The structure factors for five hydrogen-contaminated Cu_xTi_{100-x} MA samples studied previously (I) are shown with the $S(Q)$ curves for molten Cu_xTi_{100-x} alloys (after He Fenglai *et al* 1986) as an inset.

concentration function (RCF) when W_{CC} is dominant. This latter case occurs for the titanium-rich alloys. The evidence of true CSRO is a negative first peak in the RCF indicative of unlike neighbours and a strong positive second peak indicative of like-atom second neighbours. (This can also be understood in terms of Faber and Ziman (1965) partial structures since the weighting factor for Cu–Ti atomic correlations is negative and the factors for Cu–Cu and Ti–Ti correlations are positive, as explained in I.) It was found in the previous work (I) that only the RCF of the $Cu_{30}Ti_{70}$ MA specimen showed a well-developed negative first peak, but since the alloy of that composition has not amorphized fully in the present case, a direct comparison cannot be made. However, the greater height of the pre-peak in the new series of samples will influence the relative heights of the first two peaks in the RCF in the way discussed above, and this is illustrated in figure 5. The RCFs of the present

Table 1. The values of the normalized peak ratio R_N, defined in the text, are given for the present Cu_xTi_{100-x} MA amorphous alloys; the hydrogen-contaminated MA series studied previously (I); glassy Cu_xTi_{100-x} alloys (Sakata *et al* 1982) and molten Cu_xTi_{100-x} alloys (He Fenglai *et al* 1986). These values are plotted in figure 4.

Alloy	Composition	R_N	Alloy	Composition	R_N
Mechanically	$Cu_{50}Ti_{50}$	0.11	Molten	$Cu_{57}Ti_{43}$	0.21
alloyed	$Cu_{60}Ti_{40}$	0.18	alloys	$Cu_{66}Ti_{34}$	0.19
Hydrogen	$Cu_{70}Ti_{30}$	0.24		$Cu_{73}Ti_{27}$	0.22
free	$Cu_{75}Ti_{25}$	0.37		$Cu_{80}Ti_{20}$	0.19
Mechanically	$Cu_{30}Ti_{70}$	0.00	Metallic	$Cu_{35}Ti_{65}$	0.01
alloyed	$Cu_{40}Ti_{60}$	0.02	glasses	$Cu_{39}Ti_{61}$	0.04
Hydrogen	$Cu_{45}Ti_{55}$	0.03		$Cu_{43}Ti_{57}$	0.07
contaminated	$Cu_{50}Ti_{50}$	0.07		$Cu_{50}Ti_{50}$	0.16
	$Cu_{55}Ti_{45}$	0.08		$Cu_{58}Ti_{42}$	0.25
	$Cu_{60}Ti_{40}$	0.17		$Cu_{66}Ti_{34}$	0.39
	$Cu_{70}Ti_{30}$	0.18		$Cu_{70}Ti_{30}$	0.39
	$Cu_{75}Ti_{25}$	0.21			

$Cu_{60}Ti_{40}$ and $Cu_{50}Ti_{50}$ are interposed between a series of similar curves from the hydrogen-contaminated samples (I), in order to try to create a series of RCFs that show a sequence of changes as regards the relative and the absolute magnitudes of their features. It appears from this sequence that the increase in CSRO in the new hydrogen-free samples is equivalent to a shift of about 10% in composition between the first and second series. However, a more detailed statement must await a derivative of at least $S_{NN}(Q)$ and $S_{CC}(Q)$.

3.2. *Crystalline CuTi alloys*

The significant differences between the diffraction patterns of the titanium-rich crystalline alloys when examined with x-rays and with neutrons are chiefly attributable to the differences in scattering amplitude with the two radiations, which determine the visibility of the alloy constituents (table 2). It can be seen that with x-rays, copper scatters twice as effectively as titanium and one thousand times more so than hydrogen, but for neutrons, hydrogen scatters (coherently—see I) slightly better than titanium and the factor between them and copper is only five. Average values of the scattering amplitudes of the constituents of the amorphous phases can be used as a measure of their visibility. In the case of crystalline compounds suitable combinations of the scattering amplitudes, b_+ and b_-, i.e. $[xb_A \pm (100-x)b_B]/100$ give an indication of the relative intensities of fundamental and superlattice peaks.

It can be seen from table 2 that with x-rays, TiH_2 scatters only one tenth as effectively as either the amorphous alloys or the two intermetallic crystalline phases while, with neutrons, the factor is about one half. Note that with neutrons the intensities of superlattice peaks relative to fundamental peaks of the CuTi phases are the reverse of those in the x-ray case, as the negative value of b_{Ti} influences the values of b_+ and b_-. Table 2 shows that the fundamental peaks of $CuTi_2$ are virtually absent with neutrons on account of the almost complete cancellation of the scattering from one copper and two titanium nuclei. Also for TiH_2, both constituents have negative values of nuclear scattering amplitude, so the behaviour with neutrons is the same as in the x-ray case.

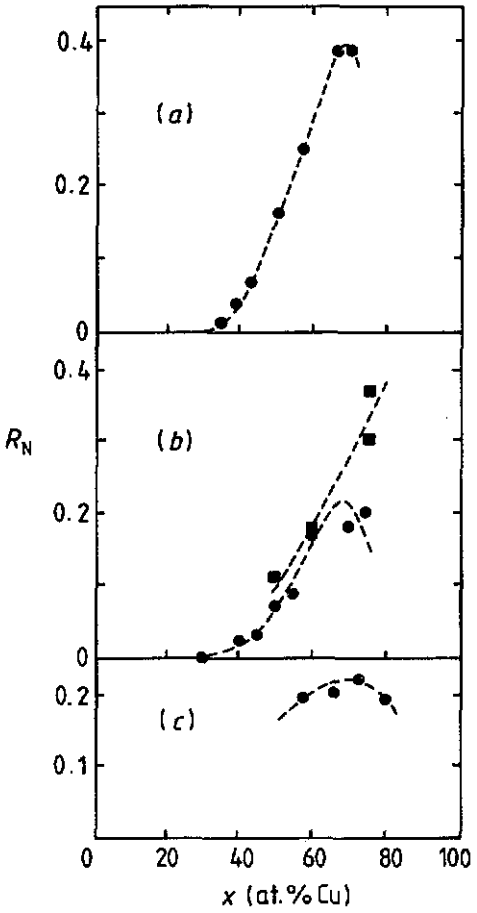

Figure 4. The normalized peak ratio R_N, defined in the text, is plotted as a function of Cu_xTi_{100-x} alloy composition: (*a*) metallic glasses; (*b*) MA samples—(■) present and (○) hydrogen contaminated (I); (*c*) molten alloys.

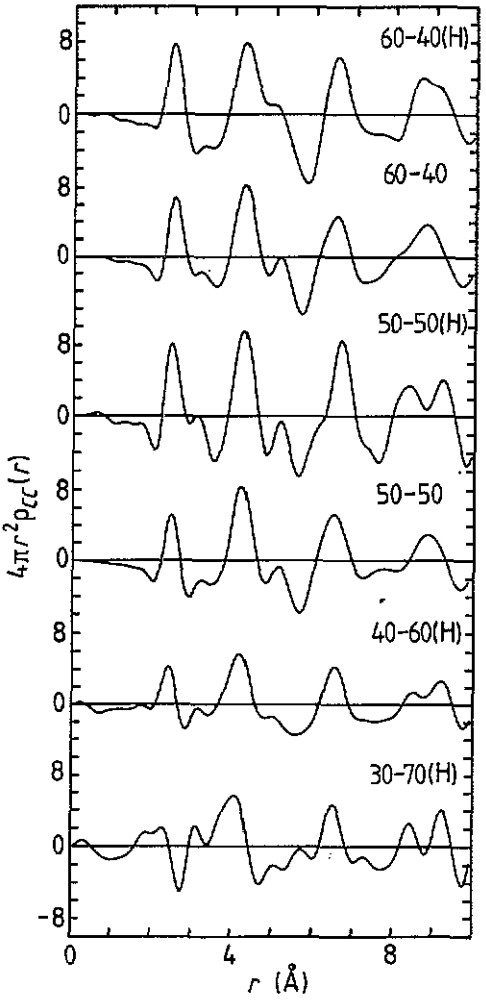

Figure 5. The radial concentration functions $4\pi r^2\rho_{CC}(r)$ for the present $Cu_{60}Ti_{40}$ and $Cu_{50}Ti_{50}$ are shown interposed between the curves of four hydrogen-contaminated specimens from the previous study (I). At any given composition the CSRO is better developed in the hydrogen-free samples. r is the radial distance.

The crystalline phases present in the titanium-rich CuTi alloys can be difficult to identify if present in a severely disordered form, contributing only indistinct features to the x-ray diffraction patterns. However, in our previous x-ray investigations (Cocco *et al* 1990a, b) the phases were identified by arresting the amorphization reaction and annealing the alloy produced. The phases present in titanium-rich alloys after MA treatment are γ-CuTi, B11-type, $P4/nmn$, a = 3.113 Å, c = 5.904 Å (Karlsson 1951) and $CuTi_2$, SiO_2-type, $I4/mmm$, a = 2.944 Å, c = 10.786 Å (Mueller and Knott 1963). In figures 6 and 7 the x-ray and neutron diffraction patterns of the titanium-rich alloys, taken from figure 1, are shown together with the simulated

Table 2. Values of the scattering amplitudes and their squares are given for copper titanium and hydrogen, for x-ray (at $Q = 0$) and neutron radiation. Average values and combinations of scattering amplitude are given to help illustrate the visibility of the amorphous and crystalline phases.

Elements	$f(0)$ (10^{-12} cm)	$f^2(0)$ (10^{-24} cm^2)	b (10^{-12} cm)	b^2 (10^{-24} cm^2)
Cu	8.17	66.74	0.7718	0.5957
Ti	6.20	38.41	−0.3438	0.1182
H	0.28	0.08	−0.3741	0.1400

Amorphous phases	$\langle f(0)^2 \rangle$ (10^{-24} cm^2)	$\langle b^2 \rangle$ (10^{-24} cm^2)
$Cu_{45}Ti_{55}$	51.16	0.3331
$Cu_{40}Ti_{60}$	49.74	0.3092
$Cu_{30}Ti_{70}$	46.91	0.2615

Crystalline phases	$f_+^2(0)$ (10^{-24} cm^2)	$f_-^2(0)$ (10^{-24} cm^2)	b_+^2 (10^{-24} cm^2)	b_-^2 (10^{-24} cm^2)
$CuTi_2$	47.01	1.99	0.001	0.237
CuTi	51.62	0.97	0.046	0.311
TiH_2	5.08	3.53	0.132	0.018

patterns for γ-CuTi and $CuTi_2$ to aid the identification of the phases. The simulation has been obtained with a conventional program for Bragg peak intensities with a provision for drawing Gaussian peaks of appropriate breadth. It can be seen that the agreement between experiment and simulation is good and that the presence of some transformed (amorphous) material in these alloys can be inferred because the background scattering is not flat, particularly in the neutron case.

4. Conclusions

This study forms part of our long-term investigation of the amorphization reaction by mechanical alloying. It has involved CuTi alloys produced using titanium powder that was essentially hydrogen free, and has led to observations that are of general interest in this field.

The first is that in the copper-rich regime, genuine amorphous alloys have been produced, but in the titanium-rich regime, the amorphization was incomplete and intermetallic compounds were observed. This suggests that hydrogen may act as a catalyst to the reaction. This is an important observation which offers a connection between amorphization by mechanical alloying and amorphization by hydrogen absorption (Yeh *et al* 1983)—for which relatively few candidates are yet known. It is possible that the fast diffusion of hydrogen through the starting materials, in addition to the asymmetric diffusion of the constituents, might assist a collapse of their crystal lattices into a disordered state via local structural relaxation. It is known, for example, that hydrogen atoms cannot occupy the favoured interstice of a Ti_4H tetrahedron unless the titanium atoms are pushed apart with an increase of the order of 6–8% in the Ti–Ti bond distance (Sidhu *et al* 1956).

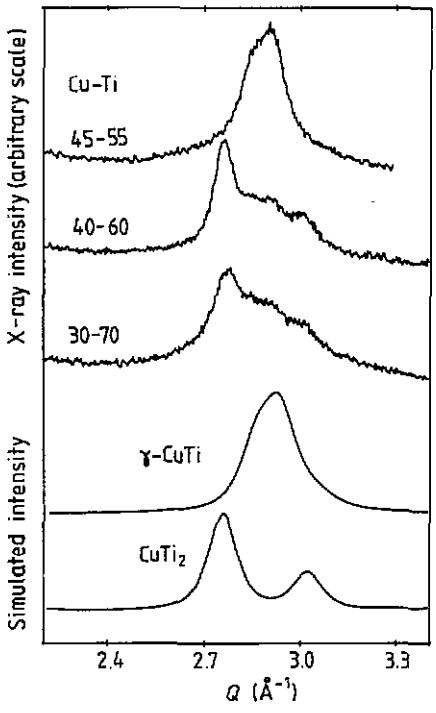

Figure 6. The x-ray diffraction patterns for the three titanium-rich Cu_xTi_{100-x} specimens from figure 1 are shown with simulated curves which identify the crystalline phases γ-CuTi and $CuTi_2$. Q is the scattering vector.

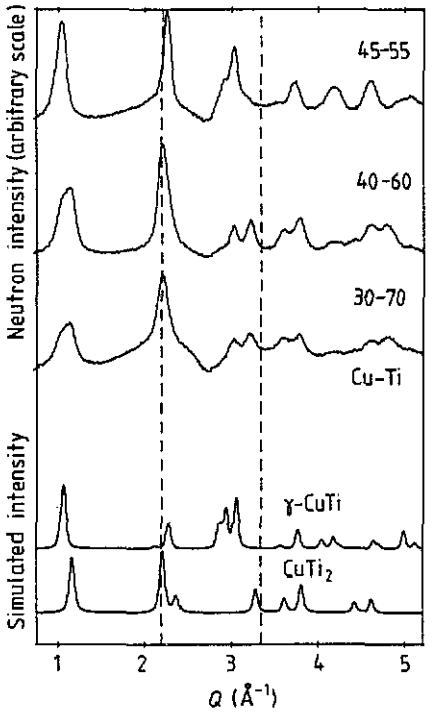

Figure 7. The neutron diffraction patterns for the three titanium-rich Cu_xTi_{100-x} specimens are shown, again with simulations for γ-CuTi and $CuTi_2$. The vertical dashed lines indicate the Q-range covered by the x-ray measurements.

Second, a comparison of the present hydrogen-free CuTi alloys and the hydrogen-contaminated series examined by us previously (I) shows that the degree of CSRO present in fully amorphous alloys can be influenced by the starting material, and specifically that the CSRO is better developed in the hydrogen-free samples. This is potentially a difficult observation to explain. Given that hydrogen atoms prefer to occupy Ti_4H tetrahedra, one might expect that the presence of hydrogen would stimulate the segregation into titanium-rich regions, through normal diffusion, rather than leading to true CSRO with unlike neighbours. In addition, as one referee has pointed out, the largest differences in the normalized peak ratio R between the two series of samples shown in figure 4(*b*) are observed for the copper-rich alloys where the hydrogen contamination is presumably smallest. A tentative explanation, which is suggested by measurements currently under way, is that in the absence of hydrogen the reaction may proceed by the creation and subsequent destruction of intermetallic phases as opposed to a direct transformation from the crystalline parents to the amorphous phase (see, e.g., Cocco *et al* 1990a, b). The CSRO present may then reflect the atomic ordering in these intermetallic phases rather than being directly related to the concentration of hydrogen present.

More generally, this observation that the CSRO present may be influenced by the starting material is quite important if it will allow the structures and the properties of the resulting alloys to be tailored to suit particular requirements. Work on metallic

alloy glasses has shown that it is sometimes necessary to choose an alloy of a given composition and then give it a special treatment to optimize a special property. One example is that of giving a structural relaxation treatment to a ferromagnetic metallic glass whose composition has already been chosen to maximise the magnetization. In the melt-spinning technique the range over which the controlling parameters can be varied is relatively narrow, because of the high quench rate required to produce a metallic glass successfully. Extensive attempts have been made to alter the degree of quenched-in CSRO in individual metallic glasses and hence their properties by heat treatments (e.g. Ruppersberg 1984) and by cold-rolling and annealing (Gardner *et al* 1985). Since these have been largely unsuccessful, this must indicate, given the sensitivity of neutron diffraction in these cases (see I for details), that the quenched-in CSRO is close to its optimum value. The possibility of varying this state in samples produced by the MA method is therefore of interest, with reference to controlling the physical properties for specific applications.

Finally, some reasons for the large differences between the x-ray and neutron diffraction patterns of identical sample materials have been discussed. These are due chiefly to the variations in the scattering amplitudes of the alloy constituents for the two radiations, complicated by the 'negative scattering' (see I) for neutrons.

Acknowledgments

This work has been supported by ENEA contract 3965 and CNR contract 89.00605.69. The collaboration between Professor Cocco and Dr Cowlam is supported by a CNR/Royal Society Travel Grant. The neutron measurements were performed with the support of the Science and Engineering Research Council and the help of Dr P Convert at ILL Grenoble. Mr Ivison acknowledges the support of an SERC studentship. A brief account of these measurements has been presented at the 7th International Conference on Rapidly Quenched Metals at Stockholm in 1990 (Ivison *et al* 1991).

References

Bhatia A B and Thornton D E 1970 *Phys. Rev.* B **2** 3004–12
Blétry J 1978 *Z. Naturf.* a **33** 327–43
Cocco G, Schiffini L, Soletta I, Baricco M and Cowlam N 1990a *J. Physique Coll.* **51** C4 175–80
Cocco G, Soletta I, Enzo S, Magini M and Cowlam N 1990b *J. Physique Coll.* **51** C4 181–7
Faber T E and Ziman J M 1965 *Phil. Mag.* **11** 153–73
Fukunaga T, Watanabe N and Suzuki K 1984 *J. Non-Cryst. Solids* **61 & 62** 343–8
Gardner P P, Cowlam N and Davies H A 1985 unpublished
He Fenglai, Cowlam N, Carr G E and Suck J-B 1986 *Phys. Chem. Liq.* **16** 99–112
Ivison P K, Cowlam N, Soletta I, Cocco G, Enzo S and Battezzati L 1991 *Mater. Sci. Eng.* A **134** 859–62
Ivison P K, Soletta I, Cowlam N, Cocco G, Enzo S and Battezzati L 1992 *J. Phys.: Condens. Matter* **4** 1635–45
Karlsson N 1951 *J. Inst. Met.* **79** 391–405
Mueller M M and Knott H W 1963 *Trans. Metall. Soc. AIME* **227** 674–8
Ruppersberg H 1984 *J. Phys. F: Met. Phys.* **14** 323–28
Ruppersberg H, Lee D and Wagner C N J 1980 *J. Phys. F: Met. Phys.* **10** 1645–52
Sakata M, Cowlam N and Davies H A 1982 *Proc. 4th Int. Conf. on Rapidly Quenched Metals* vol 1 (Sendai: Japan Institute of Metals) pp 327–9
Sidhu S S, Heaton Le Roy and Zauberis D D 1956 *Acta Crystallogr.* **9** 607–14
Yeh X L, Samwer K and Johnson W L 1983 *Appl. Phys. Lett.* **42** 242–4